# Pressure effect on hydrogen tunneling and vibrational spectrum in α-Mn

A. I. Kolesnikov,[1,*] A. Podlesnyak,[2] R. A. Sadykov,[3,4] V. E. Antonov,[5] M. A. Kuzovnikov,[5,6] G. Ehlers,[2] and G. E. Granroth[7]

[1]*Chemical and Engineering Materials Division, Oak Ridge National Laboratory, Oak Ridge, Tennessee 37831, USA*

[2]*Quantum Condensed Matter Division, Oak Ridge National Laboratory, Oak Ridge, Tennessee 37831, USA*

[3]*Institute for High Pressure Physics, RAS, 108840 Moscow, Troitsk, Russia*

[4]*Institute for Nuclear Research, RAS, 117312 Moscow, Russia*

[5]*Institute of Solid State Physics, RAS, 142432 Chernogolovka, Moscow Region, Russia*

[6]*Institute of Physical Chemistry, PAS, 01-224 Warsaw, Poland*

[7]*Neutron Data Analysis and Visualization Division, Oak Ridge National Laboratory, Oak Ridge, Tennessee 37831, USA*

(Received 29 July 2016; published 3 October 2016)

The pressure effect on the tunneling mode and vibrational spectra of hydrogen in α-$MnH_{0.07}$ has been studied by inelastic neutron scattering. Applying hydrostatic pressure of up to 30 kbar is shown to shift both the hydrogen optical modes and the tunneling peak to higher energies. First-principles calculations show that the potential for hydrogen in α-Mn becomes overall steeper with increasing pressure. At the same time, the barrier height and its extent in the direction of tunneling decrease and the calculations predict significant changes of the dynamics of hydrogen in α-Mn at 100 kbar, when the estimated tunneling splitting of the hydrogen ground state exceeds the barrier height.

DOI: 10.1103/PhysRevB.94.134301

## I. INTRODUCTION

Quantum tunneling [1,2] is a phenomenon in which a particle passes through a potential barrier when motion through that barrier is energetically forbidden by classical mechanics. Inelastic neutron scattering (INS) provides a unique method to study the vibrational and quantum tunneling dynamics of hydrogen-containing materials because of the large incoherent neutron scattering cross section of hydrogen compared to other atoms. INS studies have well demonstrated the occurrence of tunneling involving hydrogen in a number of systems, such as atomic hydrogen in metals [3–5], methyl and ammonia groups [6], and recently water in beryl [7]. Applying pressure usually leads to decreasing interatomic distances in the material and respectively increasing interatomic forces and energies of vibrational modes. The effect of pressure, on the other hand, on quantum tunneling processes is not well understood. It is known that the energy of the tunneling peaks in the INS spectra, resulting from transitions between the levels of the split ground state of the tunneling hydrogen, can increase, decrease, or remain unchanged depending on the compressed material. For example, compressing methyl iodide $CH_3I$ results in a strong (almost exponential) decrease of tunneling splitting of the methyl librational ground state from about 2.5 μeV at ambient pressure to 0.8 μeV at 3.6 kbar [8]. Application of a 3.4 kbar pressure on the tetramethylpyrazine and chloranilic acid complex at a temperature of 4.2 K results in a shift of one (out of four total) methyl rotational tunneling peak from 20.6 μeV to 12.2 μeV, while the other three tunneling peaks shift little or not at all [9], and the softening of the tunneling peak was attributed to an increase of the strength of the rotational potential. Another example is methyl tunneling in α-toluene, where two tunneling peaks were observed in the INS spectra corresponding to the two inequivalent methyl groups of this crystalline structure [10]. An application of a 4.6 kbar pressure to α-toluene results in softening of one peak (from 26.0 to 20.0 μeV) and hardening of the other one (from 28.5 to 31.7 μeV).

Our previous INS studies revealed a giant tunneling effect of hydrogen in α-Mn [11–13]. Hydrogen atoms in α-Mn ($I\bar{4}3m$ space group, 58 atoms in the cubic unit cell) occupy the 12*e*-type positions arranged in dumbbells which are 0.68 Å long. The dumbbells are located at the centers of the edges and faces of the unit cell as illustrated in Fig. 1, and each dumbbell can accommodate only one hydrogen atom. The INS spectra of α-$MnH_{0.07}$ and α-$MnD_{0.05}H_{0.005}$ displayed pronounced peaks at 6.3 and 1.6 meV, respectively. The temperature, momentum transfer, and isotopic dependencies of the peaks led to the conclusion [13] that they originated from transitions between the vibrational ground states, which are split due to the tunneling of H and D atoms between the 12*e* positions inside the dumbbells.

The pressure effect on hydrogen tunneling in α-$MnH_x$ ($x = 0.04$ and 0.07) was earlier studied by inelastic neutron scattering [14]. Hydrostatic compression to $P = 7$ kbar caused no change in the tunneling peak shape, position, nor intensity, while nonhydrostatic compression to 17 kbar completely suppressed the peak. It was also shown [14] that the intensity of the tunneling peak could be halved by grinding the $MnH_x$ sample into a fine powder. The observed reduction, and disappearance, of the tunneling peak in the INS spectra of α-$MnH_x$ was related to the residual elastic stresses (or defects) arising in the samples as a result of nonhydrostatic compression or grinding.

The present paper reports an INS study of the effect of hydrostatic pressure on the tunneling and vibrational spectra of hydrogen in α-$MnH_{0.07}$ in an extended pressure range, up to 30 kbar, and we now observe under pressure a clear shift of the tunneling peak to higher energy. To elucidate the effect of pressure on the dynamics of hydrogen in α-Mn, *ab initio* simulations were performed and the potential well for hydrogen was calculated for the conditions relevant to different pressures. Then the calculated potential well was also used to estimate the energy of tunneling splitting of the vibrational ground state of hydrogen.

*Corresponding author: kolesnikovai@ornl.gov

 

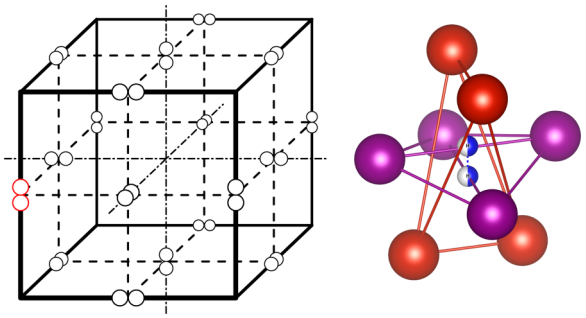

FIG. 1. The $\alpha$-Mn-H solid solution. On the left: the arrangement of dumbbells of 12*e* positions in the unit cell of $\alpha$-Mn. On the right: local structure of the hydrogen nearest neighbors; small blue-gray circles are the hydrogen atoms on 12*e* positions (50% occupancy); red and violet circles are the nearest-neighbor Mn atoms on $24g_2$ and $24g_1$ positions, respectively.

## II. EXPERIMENTAL DETAILS AND COMPUTATIONAL METHOD

The $\alpha$-$MnH_{0.07}$ solid solution was prepared by exposing $\alpha$-Mn powder to a hydrogen pressure of 8.5 kbar at 623 K for 4 h with subsequent rapid cooling to ambient temperature as described previously [11]. The content of dissolved hydrogen was determined by hot extraction into a calibrated volume.

The INS measurements were performed using the Cold Neutron Chopper Spectrometer (CNCS) [15,16] and the Fine Resolution Fermi Chopper Spectrometer (SEQUOIA) [16,17] at the Spallation Neutron Source at Oak Ridge National Laboratory. To provide an energy resolution of 1%–5% of the incident neutron energy ($E_i$), over a wide range of energy transfer ($E < 300$ meV), data were collected with different neutron energies: $E_i = 12$ meV at CNCS, and $E_i = 25,55,160,225,$ and 340 meV at SEQUOIA. Most measurements were performed at a temperature of 1.5 K using a helium cryostat at CNCS, and at 6 K using a bottom-loading closed-cycle helium refrigerator at SEQUOIA. The collected INS data were corrected for detector efficiency and transformed from the time-of-flight and instrument coordinates to the dynamic structure factor $S(Q,E)$ by using the MANTIDPLOT [18] and DAVE [19] software packages for data reduction and analysis.

A clamp piston-cylinder Ni-Cr-Al pressure cell, with an inner diameter of 4.8 mm, an outer diameter of 18 mm, and effective sample volume $\sim$0.3 $cm^3$, was used in the INS experiments up to a maximum pressure of 22 kbar (cell 1). For the experiments at 30 kbar, a similar pressure cell (with a slightly conical outer cylinder profile) was inserted into an aluminum-alloy V96 supporting cylinder of an 80 mm outer diameter (cell 2). About 1.4 g of $\alpha$-$MnH_{0.07}$ powder was mixed with fluorinert liquid (used as pressure-transmitting medium) and pressurized to 16 and 22 kbar (cell 1), and to 30 kbar (cell 2). To quantify the background signal from the pressure cell, INS spectra were also measured with the pressure cells filled with the fluorinert liquid (without $\alpha$-$MnH_{0.07}$ powder) at ambient pressure and the same temperatures and incident energies $E_i$.

First-principles calculations were performed using the Vienna *ab initio* simulation package (VASP) [20] based on projector augmented wave (PAW) pseudopotentials [21] within the generalized gradient approximation (GGA) as parametrized by Perdew, Burke, and Ernzerhof (PBE) [22]. After careful convergence tests, a plane-wave cutoff energy of 350 eV and 9 $\times$9$\times$ 9 *k*-point Monkhorst-Pack mesh [23] were found to be sufficient to converge the total energy within 1 meV per cell.

The crystal structure of the body-centered cubic unit cell of $\alpha$-Mn (containing 58 atoms of manganese) with one hydrogen atom at a 12*e*-type position in the center of the unit cell (all atomic coordinates were taken from Ref. [11]) was optimized allowing the unit cell parameter and atomic coordinates to vary. Since calculations of the noncollinear magnetic structure and related tetragonal distortions in $\alpha$-Mn are ambiguous [24], we limited our DFT study to consider the nonmagnetic cubic structure only. This resulted in a 10% smaller theoretical equilibrium volume ($a_{calc} = 8.5437$ Å compared to $a_{exp} = 8.865$ Å), in agreement with previous calculations [24]. For the high-pressure simulations the lattice parameter was fixed (we used the calculated $a_{calc}$, reduced according to the experimental volume reduction of pure $\alpha$-Mn under pressure [25]), and only atomic coordinates were varied.

## III. RESULTS AND DISCUSSION

Figure 2 shows the INS spectra of $\alpha$-$MnH_{0.07}$ in the energy range of the hydrogen tunneling peak (around 6 meV) at hydrostatic pressures 1 bar, 16, 22, and 30 kbar, all at $T = 1.5$ K. The raw data and the $(Q,E)$ contour plots of the INS data are shown in the Supplemental Material [26]. Two Gaussian functions and a sloped linear background are fitted to the tunneling peak. A possible reason for the splitting of the observed tunneling peak can be a tetragonal distortion of the crystal structure of $\alpha$-Mn in the antiferromagnetic state (space group $I\bar{4}2m$ at temperatures below the Néel temperature of $T_N = 95$ K for pure $\alpha$-Mn and $T_N = 140$ K for $\alpha$-$MnH_{0.07}$). The tetragonal distortion of the unit cell, $a/c = 1.00035$,

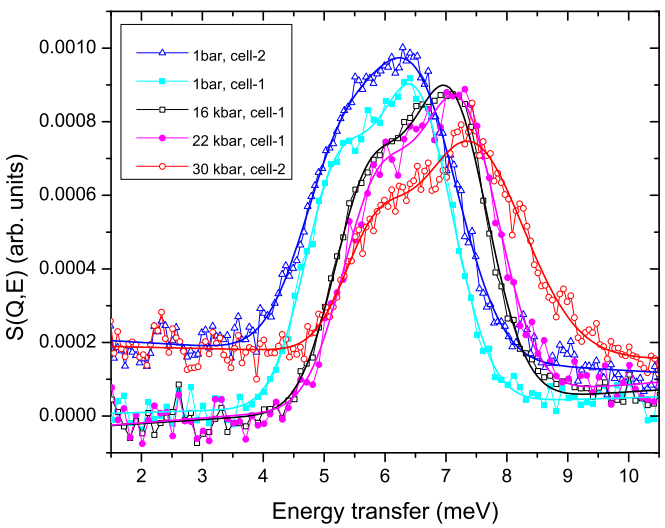


FIG. 2. INS spectra of $\alpha$-$MnH_{0.07}$ measured at $T = 1.5$ K and different pressures using the CNCS spectrometer with $E_i = 12$ meV; the background from the high-pressure cell and the cryostat has been subtracted from the data.

TABLE I. Energy positions ($E_{t1}$ and $E_{t2}$) and intensity ratios $I_{t2}/I_{t1}$ of the Gaussian peaks used to fit the tunneling peak in the INS spectra of $\alpha$-$MnH_{0.07}$ measured at different pressures ($P$). The value of the average tunneling peak shift, $\Delta E = \langle E_t(P)\rangle - \langle E_t(P = 1\text{ bar})\rangle$, and its relative value $\delta = \Delta E/\langle E_t(P = 1\text{ bar})\rangle$ are also presented; all energies are in meV.

| cells | $P$ | $E_{t1}$ | $E_{t2}$ | $I_{t2}/I_{t1}$ | $\Delta E$ | $\delta$ |
|---|---|---|---|---|---|---|
| cell 1 | 1 bar | 5.19 | 6.49 | 1.7 | | |
| cell 2 | 1 bar | 5.17 | 6.43 | 2.5 | | |
| cell 1 | 16 kbar | 5.75 | 7.09 | 1.4 | 0.580 | 9.9% |
| cell 1 | 22 kbar | 5.91 | 7.26 | 1.4 | 0.745 | 12.8% |
| cell 2 | 30 kbar | 5.80 | 7.38 | 3.9 | 0.790 | 13.6% |

is small [27], but the changes of the Mn atomic positions under distortion are maximal for the $24g_2$ sites, which are the nearest neighbors of the H atom and play the leading role in the construction of the hydrogen potential. If the splitting is indeed caused by the tetragonal distortion, the intensity ratio of the split components of the tunneling peak should be 2:1. The values of this intensity ratio, obtained from the fit of the experimental $S(Q,E)$ data (see Table I) are reasonably close to this value. The observed uncertainties of the intensity ratio are largely due to the cross correlation with fit parameters describing the linearly sloped background. An independent measurement on $\alpha$-$MnH_{0.07}$, conducted with a larger sample and without the high-pressure cell [13] (therefore less affected by background), gave an intensity ratio of about 2, supporting the distortive origin of the splitting (see Fig. S4 in the Supplemental Material [26]).

The position of the tunneling peak shifts to higher energy with increasing pressure (see details in Table I), and at $P = 30$ kbar the shift reaches 13.6% of its value at ambient pressure. The intensity of the tunneling peak and its shape are almost unaffected by the pressure change. The shifts of the hydrogen fundamental optical peaks, with applied pressures of 16 and 22 kbar, are about 1–2 meV (Fig. 3). Therefore the relative shifts of the optical peaks are significantly smaller than the relative shift of the tunneling peak (see Table II). The increase in the optical peak energy with the pressure increase indicates a stiffening of the potential well for hydrogen in $\alpha$-Mn, while the positive shift of the position of the tunneling peak means that the barrier in the double-well potential in the direction of hydrogen tunneling decreases with pressure. Using the experimental values of volume reduction of $\alpha$-Mn under pressure [25] and assuming a similar behavior for $\alpha$-$MnH_{0.07}$, we calculated the Grüneisen parameters for the observed peaks in the INS spectra of $\alpha$-$MnH_{0.07}$ at different pressures with

TABLE II. Energy positions of the hydrogen fundamental optical modes ($E_{1,2,3}$) in the INS spectra of $\alpha$-$MnH_{0.07}$ measured at different pressures ($P$); all energies are in meV.

| $P$ | $E_1$ | $E_2$ | $E_3$ |
|---|---|---|---|
| 1 bar | 73.3 | 106.0 | 131.3 |
| 16 kbar | 74.4 | 107.5 | 132.5 |
| 22 kbar | 74.3 | 108.0 | 132.8 |

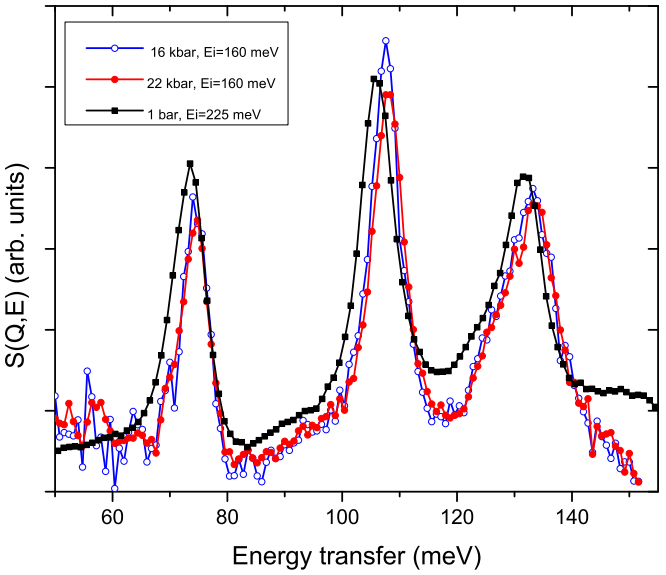


FIG. 3. INS spectra of $\alpha$-$MnH_{0.07}$ measured at $T = 5$ K and pressures of 16 and 22 kbar using the SEQUOIA spectrometer with $E_i = 160$ meV; the background from the high-pressure cell has been subtracted from the data. The spectrum for $\alpha$-$MnH_{0.07}$ at ambient pressure was measured without the pressure cell using $E_i = 225$ meV.

an expression $\gamma_i = -\partial \ln E_i/\partial \ln V$. The obtained Grüneisen parameters (Table III) for the tunneling modes are about an order of magnitude larger than for the optical modes, and all $\gamma_i$ parameters decrease with increasing pressure.

The 3D potential for hydrogen in $\alpha$-Mn calculated for ambient pressure (Fig. 4) shows a relatively shallow double-well profile along the dumbbell, and steeper single-well in the perpendicular $ab$ plane. Note that in the $ab$ plane the potential is anisotropic and changes its stiffness between the $(x,x)$ and $(x,-x)$ directions when hydrogen moves (tunnels) from one side of the dumbbell to another. The calculated energies of the hydrogen optical modes in these directions (in the single-well potential) are 152.2 meV and 110.3 meV, respectively; the optical mode in the double-well potential has an energy of 75.3 meV. All these energies are in good agreement with experimental observations (Table II). Figure 5 displays 1D profiles of the double-well potential calculated for pressures 1 bar and 30 kbar used in the experiment, and also for much higher pressures of 100 kbar and 1 Mbar, which are not currently accessible with inelastic neutron scattering. The barrier height decreases from 16.9 meV at ambient pressure to 15.2 meV at 30 kbar, 3.1 meV at 100 kbar, and 0.2 meV at

TABLE III. Grüneisen parameters $\gamma_i$ for the peaks observed in the INS spectra of $\alpha$-$MnH_{0.07}$ at different pressures.

| $E_i$ (meV) | $P = 16$ kbar | $P = 22$ kbar | $P = 30$ kbar |
|---|---|---|---|
| 6 | 7.49 | 7.04 | 5.49 |
| 73 | 1.13 | 0.75 | |
| 106 | 1.07 | 1.04 | |
| 131 | 0.69 | 0.63 | |
| 190 | 1.08 | 0.93 | |

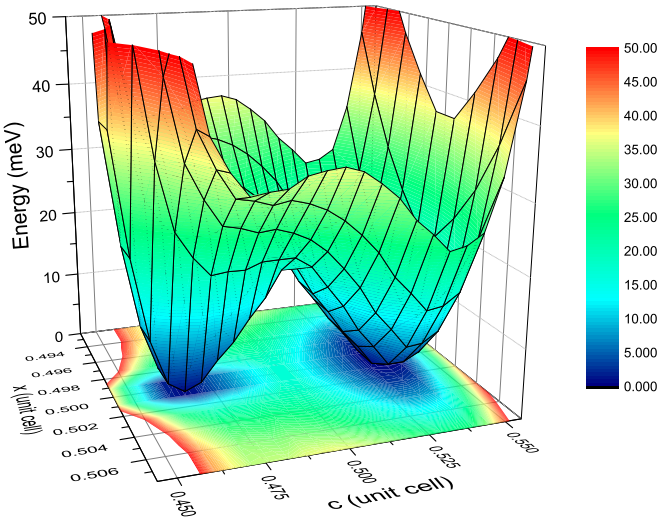


FIG. 4. Calculated 3D potential for a hydrogen atom in $\alpha$-Mn, cut over the (110) plane at the dumbbell placed along the $c$ axis; the distances are in the unit cell parameter units.

1 Mbar. The fractional coordinates of the minima $(0.5 \pm l)$ are also changed, $l = 0.0330$, 0.0306, 0.0222, and 0.0070 for $P = 1$ bar, 30 kbar, 100 kbar, and 1 Mbar, respectively, resulting in a significant decrease of the dumbbell length, from 0.56 Å at 1 bar to 0.34 Å at 100 kbar. The calculations show that at 1 Mbar the potential can be considered a single-well potential.

The tunneling splitting of the ground state for hydrogen in the double-well potential $U(x)$ can be calculated by using the expression [28]

$$E_t^{calc} = \frac{E_1}{\pi} \exp\left(-\frac{1}{\hbar}\int \sqrt{2m[U(x) - E_G]}\, dx\right), \quad (1)$$

where $E_G$ and $E_1$ are the energy of the hydrogen ground state and optical mode, respectively, in the direction of tunneling,

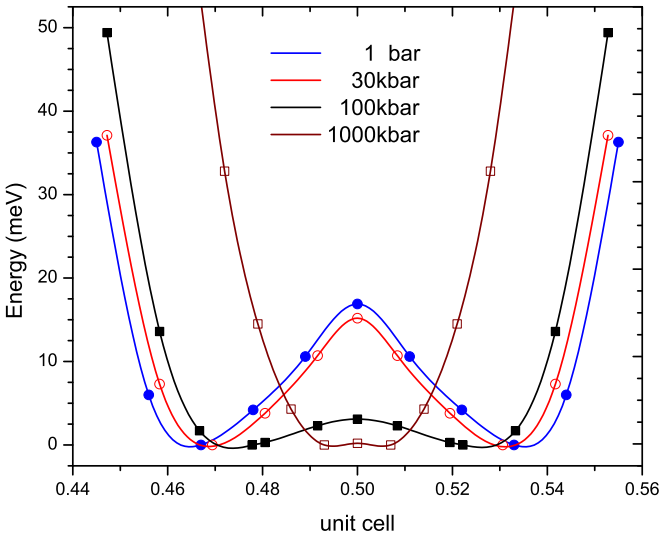


FIG. 5. Double-well potential for a hydrogen atom in $\alpha$-Mn along the dumbbell calculated for different pressures; the distance is in the unit cell parameter units.

$m$ is the mass of the hydrogen atom, and the integral should be taken under the barrier, between the turning points of the hydrogen. Because our DFT simulations are limited to the nonmagnetic cubic structure, the calculated dumbbell length is about 20% smaller than the experimental value and the obtained potential barrier is underestimated. Since the calculated potential does not include quantum fluctuations, which could significantly modify the energy of the ground state, for estimation of the tunneling splitting we used $E_G = 0$, and the integration in Eq. (1) was made between the minima points of the potential. The calculated tunneling splittings are $E_t^{calc} = 8.5$ meV at ambient pressure, 10.3 meV for $P = 30$ kbar, and 17.5 meV for $P = 100$ kbar. The first two values are in qualitative agreement with the experimental data (see Table I), giving a relative shift of the tunneling peak of $\delta = 21.1\%$ for $P = 30$ kbar. We do not have the experimental data for tunneling splitting at $P = 100$ kbar, but the calculated value $E_t = 17.5$ meV is larger than the barrier height, which is only 3.1 meV, and the use of Eq. (1) for this pressure would not be correct. Therefore the dynamics of hydrogen in $\alpha$-Mn at $P = 100$ kbar should be significantly different than at pressures below 30 kbar.

## IV. CONCLUSIONS

In summary, we have measured INS spectra of $\alpha$-$MnH_{0.07}$ under hydrostatic pressures up to $P = 30$ kbar. The observed hydrogen optical modes and tunneling mode progressively shift to higher energies, while all Grüneisen parameters decrease with increasing pressure. The first-principles calculations predict a 3D potential with a double-well shape in the direction of hydrogen tunneling, and describe the experimental data reasonably well. Both experiment and calculations reveal that an increase of pressure results in an increase of the potential stiffness and a decrease of the barrier for hydrogen tunneling. The calculations show that at $P = 100$ kbar the dynamics of hydrogen in $\alpha$-Mn should be significantly changed due to the expected monotonic decrease of the barrier with increasing pressure, and at $P = 1$ Mbar the potential can be considered a single-well potential.

## ACKNOWLEDGMENTS

Research at Oak Ridge National Laboratory's Spallation Neutron Source was supported by the Scientific User Facilities Division, Office of Basic Energy Sciences, U.S. Department of Energy. This research used resources of the National Energy Research Scientific Computing Center, which is supported by the Office of Science of the U.S. Department of Energy under Contract No. DE-AC02-05CH11231. A portion of this research was sponsored by the Laboratory Directed Research and Development Program of Oak Ridge National Laboratory, managed by UT-Battelle, LLC, for the U.S. Department of Energy. Support by a grant of the Program on Elementary Particle Physics, Fundamental Nuclear Physics, and Nuclear Technologies of RAS is also acknowledged.

This manuscript has been authored by UT-Battelle, LLC, under Contract No. DE-AC05-00OR22725 with the U.S. Department of Energy. The United States Government retains and the publisher, by accepting the article for publication,

[1] V. Narayanamurti and R. O. Pohl, Tunneling states of defects in solids, Rev. Mod. Phys. **42**, 201 (1970).

[2] V. I. Goldanskii, Facts and hypotheses of molecular chemical tunneling, Nature (London) **279**, 109 (1979).

[3] H. Wipf, A. Magerl, S. M. Shapiro, S. K. Satija, and W. Thomlinson, Neutron-Spectroscopic Evidence for Hydrogen Tunneling States in Niobium, Phys. Rev. Lett. **46**, 947 (1981).

[4] A. Magerl, A. J. Dianoux, H. Wipf, K. Neumaier, and I. S. Anderson, Concentration Dependence and Temperature Dependence of Hydrogen Tunneling in $Nb(OH)_x$, Phys. Rev. Lett. **56**, 159 (1986).

[5] H. Grabert and H. Wipf, Tunneling of hydrogen in metals, *Festkörperprobleme 30*, Advances in Solid State Physics, Vol. 30, edited by U. Rössler (Springer, Berlin, Heidelberg, 1990), pp. 1–23.

[6] M. Prager and A. Heidemann, Rotational tunneling and neutron spectroscopy: A compilation, Chem. Rev. **97**, 2933 (1997).

[7] A. I. Kolesnikov, G. F. Reiter, N. Choudhury, T. R. Prisk, E. Mamontov, A. Podlesnyak, G. Ehlers, A. G. Seel, D. J. Wesolowski, and L. M. Anovitz, Quantum Tunneling of Water in Beryl: A New State of Water Molecule, Phys. Rev. Lett. **116**, 167802 (2016).

[8] M. Prager, C. Vettier, and S. Mahling-Ennanoui, The temperature dependence of the methyl rotational potential in methyl iodide under pressure, Z. Phys. B **75**, 217 (1989).

[9] M. Prager, A. Pietraszko, L. Sobczyk, E. Grech, T. Seydel, A. Wischnewski, and M. Zamponi, X-ray diffraction and inelastic neutron scattering study of 1:1 tetramethylpyrazine chloranilic acid complex: Temperature, isotope, and pressure effects, J. Chem. Phys. **125**, 194525 (2006).

[10] D. Cavagnat, A. Magerl, C. Vettier, and S. Clough, Methyl tunnelling in $\alpha$-crystallized toluene by inelastic neutron scattering: Temperature and pressure effects, J. Phys. C **19**, 6665 (1986).

[11] V. K. Fedotov, V. E. Antonov, K. Cornell, G. Grosse, A. I. Kolesnikov, V. V. Sikolenko, V. V. Sumin, F. E. Wagner, and H. Wipf, Neutron scattering studies of the structure and lattice dynamics of a solid solution of hydrogen in alpha-manganese, J. Phys.: Condens. Matter **10**, 5255 (1998).

[12] V. E. Antonov, B. Dorner, V. K. Fedotov, G. Grosse, A. S. Ivanov, A. I. Kolesnikov, V. V. Sikolenko, and F. E. Wagner, Giant tunnelling effect of hydrogen and deuterium in $\alpha$-manganese, J. Alloys Compd. **330–332**, 462 (2002).

[13] A. I. Kolesnikov, V. E. Antonov, S. M. Bennington, B. Dorner, V. K. Fedotov, G. Grosse, J. C. Li, S. F. Parker, and F. E. Wagner, The vibrational spectrum and giant tunnelling effect of hydrogen dissolved in alpha-Mn, Physica B **263–264**, 421 (1999).

[14] V. E. Antonov, V. P. Glazkov, D. P. Kozlenko, B. N. Savenko, V. A. Somenkov, and V. K. Fedotov, Hydrogen tunneling modes in $\alpha$-Mn suppressed by elastic stresses, JETP Lett. **76**, 318 (2002).

[15] G. Ehlers, A. Podlesnyak, J. L. Niedziela, E. B. Iverson, and P. E. Sokol, The new cold neutron chopper spectrometer at the Spallation Neutron Source: Design and performance, Rev. Sci. Instrum. **82**, 085108 (2011).

[16] M. B. Stone, J. L. Niedziela, D. L. Abernathy, L. DeBeer-Schmitt, G. Ehlers, O. Garlea, G. E. Granroth, M. Graves-Brook, A. I. Kolesnikov, A. Podlesnyak, and B. Winn, A comparison of four direct geometry time-of-fight spectrometers at the Spallation Neutron Source, Rev. Sci. Instrum. **85**, 045113 (2014).

[17] G. E. Granroth, A. I. Kolesnikov, T. E. Sherline, J. P. Clancy, K. A. Ross, J. P. C. Ruff, B. D. Gaulin, and S. E. Nagler, SEQUOIA: A newly operating chopper spectrometer at the SNS, J. Phys.: Conf. Ser. **251**, 012058 (2010).

[18] O. Arnold, J. C. Bilheux, J. M. Borreguero, A. Buts, S. I. Campbell, L. Chapon, M. Doucet, N. Draper, R. Ferraz Leal, M. A. Gigg, V. E. Lynch, A. Markvardsen, D. J. Mikkelson, R. L. Mikkelson, R. Miller *et al.*, Mantid—Data analysis and visualization package for neutron scattering and $\mu$ SR experiments, Nucl. Instrum. Methods Phys. Res., Sect. A **764**, 156 (2014).

[19] R. T. Azuah, L. R. Kneller, Y. Qiu, P. L. W. Tregenna-Piggott, C. M. Brown, J. R. D. Copley, and R. M. Dimeo, DAVE: A comprehensive software suite for the reduction, visualization, and analysis of low energy neutron spectroscopic data, J. Res. Natl. Inst. Stand. Technol. **114**, 341 (2009).

[20] G. Kresse and J. Furthmüller, Efficient iterative schemes for *ab initio* total-energy calculations using a plane-wave basis set, Phys. Rev. B **54**, 11169 (1996).

[21] G. Kresse and D. Joubert, From ultrasoft pseudopotentials to the projector augmented-wave method, Phys. Rev. B **59**, 1758 (1999).

[22] J. P. Perdew, K. Burke, and M. Ernzerhof, Generalized Gradient Approximation Made Simple, Phys. Rev. Lett. **77**, 3865 (1996).

[23] H. J. Monkhorst and J. D. Pack, Special points for Brillouin-zone integrations, Phys. Rev. B **13**, 5188 (1976).

[24] D. Hobbs, J. Hafner, and D. Spišák, Understanding the complex metallic element Mn. I. Crystalline and noncollinear magnetic structure of $\alpha$-Mn, Phys. Rev. B **68**, 014407 (2003).

[25] H. Fujihisa and K. Takemura, Stability and the equation of state of $\alpha$-manganese under ultrahigh pressure, Phys. Rev. B **52**, 13257 (1995).

[26] See Supplemental Material at http://link.aps.org/supplemental/10.1103/PhysRevB.94.134301 for the raw INS spectra and the $(Q,E)$ contour plots of the INS data for $\alpha$-$MnH_{0.07}$ measured under high pressure.

[27] A. C. Lawson, A. C. Larson, M. C. Aronson, S. Johnson, Z. Fisk, P. C. Canfield, J. D. Thompson, and R. B. Von Dreele, Magnetic and crystallographic order in $\alpha$-manganese, J. Appl. Phys. **76**, 7049 (1994).

[28] L. D. Landau and E. M. Lifshitz, *Quantum Mechanics: Non-Relativistic Theory*, Vol. 3 of A Course of Theoretical Physics, 2nd ed. (Pergamon Press, Oxford, 1965), p. 176.